A System-Level Multi-Objective Framework for Solar Tracking with Chaotic ABC MPPT

Justin London[1], Tingjun Lei[1,*], Lin Gong[2], Guoming Li[3], and Chaomin Luo[4]
[1]*School of Electrical Engineering and Computer Science, University of North Dakota, Grand Forks, ND, USA*
[2]*Department of Electrical and Computer Engineering, Prairie View A&M University, Prairie View, TX, USA*
[3]*Department of Poultry Science, University of Georgia, Athens, GA, USA*
[4]*Department of Electrical and Computer Engineering, Mississippi State University, Mississippi State, MS, USA*
[*]Corresponding Author: Tingjun Lei, *Senior Member, IEEE*, Email: Tingjun.Lei@UND.edu.

***Abstract*—Solar tracking systems operating in dynamic and partially shaded environments require not only effective maximum power point tracking (MPPT) but also system-level trade-offs among energy yield, tracking accuracy, and control effort. Most existing approaches address MPPT or mechanical tracking optimization in isolation, lacking an integrated formulation that captures these competing objectives within a unified framework. In this paper, solar tracking is formulated as a system-level multi-objective optimization problem, and a hierarchical optimization framework is proposed in which a Chaotic Artificial Bee Colony (CABC)-based MPPT controller is integrated as an inner-loop power optimization mechanism. The outer-loop optimization explicitly accounts for multiple competing objectives, including power maximization, tracking stability, and control performance, subject to physical and operational constraints of a multi-axis solar tracking system. The proposed framework is evaluated through simulation and experimental studies. Results show that the CABC-based MPPT improves convergence and reduces steady-state oscillations under dynamic irradiance and partial shading conditions, while system-level multi-objective optimization demonstrates Pareto trade-offs across competing performance metrics.**

***Index Terms*—photovoltaic; DC motor; stepper motor; solar tracker; control systems; water pumping; agriculture; autonomous robots; energy; swarm intelligence;**

I. Introduction

Solar tracking systems play a critical role in improving the energy yield of photovoltaic (PV) installations by continuously aligning solar panels with incident sunlight [1]. In practice, however, solar tracking systems operate under highly dynamic conditions, including time-varying irradiance, partial shading, and environmental disturbances, which introduce significant challenges for both control and optimization. In addition to maximizing harvested power, practical solar tracking systems must balance competing objectives such as tracking accuracy, stability, and control effort, particularly for portable and multi-axis configurations with physical and operational constraints.

Maximum power point tracking (MPPT) has been extensively studied as a key component of PV systems, with conventional techniques such as incremental conductance (IC) remaining widely used due to their simplicity. Nevertheless, these methods often suffer from steady-state oscillations and degraded performance under rapidly changing irradiance or partial shading conditions, where multiple local optima may exist in the power-voltage characteristic. To address these limitations, population-based and evolutionary optimization methods have been increasingly explored for MPPT, owing to their global search capability and robustness to nonlinearity. Despite their advantages, most existing MPPT-oriented studies treat power optimization as an isolated problem, without explicitly considering its interaction with higher-level tracking and control objectives at the system level. Meanwhile, multi-axis solar tracking systems have been investigated from mechanical design and control perspectives, including trajectory planning, actuator coordination, and tracking accuracy optimization. Multi-objective optimization techniques have been applied to solar energy systems to capture trade-offs among competing performance metrics. However, many of these studies focus on system-level optimization alone or rely on simplified power models, while assuming idealized or fixed MPPT behavior. As a result, the coupling between inner-loop power optimization and outer-loop system-level objectives is often neglected, limiting the applicability of such approaches under realistic operating conditions.

Motivated by these observations, solar tracking is formulated in this work as a system-level multi-objective optimization problem, in which power generation, tracking performance, and control-related objectives are simultaneously considered under physical and operational constraints. To address this problem, a hierarchical optimization framework is proposed that integrates a Chaotic Artificial Bee Colony (CABC)-based MPPT controller as an inner-loop power optimization mechanism. The chaotic enhancement enables improved exploration capability and convergence behavior in complex and partially shaded environments, while the outer-loop multi-objective formulation explicitly captures trade-offs among competing system-level objectives. The system-level multi-objective formulation reveals clear Pareto trade-offs among competing performance metrics, and hardware experiments conducted on a portable multi-axis solar tracking prototype confirm the practical feasibility of the proposed approach. The main contributions of this work are summarized as follows:

(1) A system-level multi-objective formulation of solar tracking is developed, in which power generation, tracking performance, and control-related objectives are jointly optimized under physical and operational constraints of

a multi-axis tracking system.

(2) A hierarchical optimization framework is proposed that explicitly couples system-level multi-objective optimization with inner-loop power control, enabling coordinated optimization between high-level tracking objectives and real-time MPPT behavior.

(3) A Chaotic Artificial Bee Colony (CABC)-based MPPT strategy is designed as the inner-loop optimizer, enhancing global search capability and convergence robustness under dynamic irradiance and partial shading conditions.

II. Related Work

Research on solar tracking spans mechanical configurations, sensing modalities, and control strategies, with single-/dual-/multi-axis trackers being widely reviewed and compared in terms of energy yield, cost, and practical constraints. Recent surveys summarize the design space and highlight that real-world performance is strongly shaped by actuator limits, stability requirements, and deployment conditions rather than geometry alone [2]–[4]. On the sensing and implementation side, dedicated sun-sensing solutions and sensor-driven trackers have been developed to improve tracking accuracy and robustness, including filtered sun sensors for high-precision tracking and related deployment in solar applications [5], [6], as well as practical dual-axis tracking prototypes and performance analyses [7], [8]. These works collectively indicate that tracking should be treated as a closed-loop system problem, where alignment accuracy and control effort must be balanced under physical constraints. MPPT remains essential for PV systems, and its performance can degrade significantly under dynamic irradiance and partial shading, where power characteristics may become multi-modal. Partial shading has been repeatedly recognized as a major source of PV performance loss in practical systems [9]. Beyond conventional MPPT, evolutionary computation and swarm intelligence have been increasingly adopted to improve robustness in non-convex operating conditions. For example, adaptive Particle Swarm Optimization (PSO) strategies have been studied for MPPT with explicit comparisons across inertia-weight and acceleration-coefficient designs [10], [11]. Such evidence motivates embedded population-based MPPT for handling multi-peak landscapes induced by partial shading.

Multi-objective optimization has also gained increasing attention in energy-related applications for explicitly representing trade-offs among competing metrics [11]–[14]. Representative studies apply intelligent algorithms to obtain Pareto-optimal solutions and analyze sensitivity in integrated solar-energy design problems [15]. From an evolutionary computation perspective, multi-objective formulations and swarm-based mechanisms have been used to expose Pareto trade-offs and support operating-point selection in complex systems [16]–[18]. Related swarm-intelligence variants further demonstrate the practicality of population-based search in dynamic, constraint-rich environments [19]–[25].

Despite these advances, much of the existing literature still addresses MPPT or tracker-level control in isolation, or assumes idealized MPPT behavior when system-level optimization is performed. This decoupling can be limiting because the system-level energy objective depends on the closed-loop interaction between tracking dynamics, constraints, and MPPT response, especially under partial shading and time-varying irradiance. Different from prior work, this paper integrates these aspects through a hierarchical structure: solar tracking is formulated as a system-level multi-objective optimization problem, and a CABC-based MPPT is embedded as the inner-loop power optimizer. This design enables Pareto trade-off analysis to be conducted using power outputs generated by an explicit MPPT process, thereby capturing realistic couplings among power maximization, tracking performance, and control effort under realistic operating conditions.

III. System Model and Multi-Objective Problem Formulation

A. System Overview and Solar-Geometry Definitions

A portable multi-axis solar tracking system is considered, in which a PV module is mounted on a motorized tracking mechanism with multiple rotational degrees of freedom. The system continuously adjusts the panel orientation to improve incident irradiance under time-varying weather, partial shading, actuator limits, and environmental disturbances. The overall control architecture follows a hierarchical structure: an inner-loop MPPT controller regulates the electrical operating point of the PV module for instantaneous power maximization, while the outer-loop tracking controller governs the mechanical alignment behavior and associated control effort.

To define tracking performance, standard solar position angles are used. As illustrated in Fig. 1, the solar elevation angle θ_{SE} describes the angle between the sun and the local horizon, the solar zenith angle θ_{SZ} is its complement, and the solar azimuth angle θ_{SA} specifies the sun direction around the horizon. These angles are used to characterize the desired panel orientation and quantify tracking error through the angle-of-incidence (AOI) relationship.

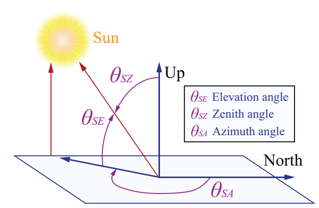

Fig. 1. Solar position angles used in this paper: elevation θ_{SE}, zenith θ_{SZ}, and azimuth θ_{SA} (measured clockwise from true north). These definitions support the solar angle-of-incidence and tracking-error formulations.

Let θ_{TE} and θ_{TA} denote the tracker elevation and azimuth angles, respectively. The solar angle of incidence (AOI), $\alpha \in [0, 90)$, is defined as the angle between the PV panel normal vector and the sun direction vector. Following the standard azimuth-elevation geometry, AOI can be denoted as

$$\alpha = \cos^{-1}\Big(\sin(\theta_{SE})\sin(\theta_{TE}) + \cos(\theta_{SE})\cos(\theta_{TE}) \cdot \cos(\theta_{SA} - \theta_{TA}) \Big). \tag{1}$$

A smaller AOI indicates better alignment and typically yields higher effective irradiance on the panel surface. Let $\mathbf{x} \in \mathbb{R}^n$ denote the vector of system-level decision variables. In this work, $\mathbf{x}$ represents the operating and control parameters that determine the tracker response, such as tracker motion parameters, controller parameters (e.g., gains or damping-related terms), and other system-level settings that affect the interaction between mechanical tracking and inner-loop MPPT behavior. The formulation is intentionally kept general to accommodate different tracker configurations and implementations. All decision variables are constrained by physical and operational limits. Let Ω denote the feasible set induced by actuator saturation, allowable angle ranges, rate limits, and safety constraints. The optimization is performed over $\mathbf{x} \in \Omega$ to ensure that candidate solutions remain physically realizable and practically deployable.

B. System-Level Multi-Objective Optimization Formulation

Solar tracking is formulated as a system-level multi-objective optimization problem that captures competing performance requirements. For a given operating horizon $[0, T]$, the following objectives are considered.

(a) Energy/power objective. The primary objective is to maximize the harvested energy (equivalently, the average power). Using a minimization convention,

$$f_1(\mathbf{x}) = -\frac{1}{T}\int_0^T P(t;\mathbf{x})\, dt, \tag{2}$$

where $P(t;\mathbf{x})$ denotes the instantaneous PV output power regulated by the inner-loop MPPT controller under the system-level setting $\mathbf{x}$.

(b) Tracking accuracy objective. Tracking quality is quantified through the AOI (or an AOI-derived error metric). A representative objective is

$$f_2(\mathbf{x}) = \frac{1}{T}\int_0^T \alpha(t;\mathbf{x})\, dt, \tag{3}$$

where $\alpha(t;\mathbf{x})$ is computed from (1). This objective penalizes persistent misalignment between the panel orientation and the sun direction.

(c) Control-effort/stability objective. To limit actuator usage and promote stable motion, control effort is penalized via

$$f_3(\mathbf{x}) = \frac{1}{T}\int_0^T \|u(t;\mathbf{x})\|^2\, dt, \tag{4}$$

where $u(t;\mathbf{x})$ denotes the actuator control input (or a proxy such as motor command/current). This term discourages aggressive or oscillatory behavior that may improve alignment but increases mechanical wear and energy consumption.

The system-level multi-objective problem is therefore expressed as

$$\min_{\mathbf{x}\in\Omega}\ \mathbf{f}(\mathbf{x}) = \left[f_1(\mathbf{x}),\ f_2(\mathbf{x}),\ f_3(\mathbf{x})\right]. \tag{5}$$

Rather than yielding a single optimum, (5) produces a set of Pareto-optimal solutions that explicitly characterize trade-offs among power generation, tracking accuracy, and control effort. In the proposed hierarchical framework, the inner-loop MPPT determines the electrical operating point and thus directly influences $P(t;\mathbf{x})$ in (2), while the outer-loop settings $\mathbf{x}$ govern tracking dynamics and the competing objectives in (3) and (4). The specific inner-loop implementation using a CABC strategy and the resulting optimization procedure are detailed in the following section.

IV. Hierarchical Optimization Framework

This section presents a hierarchical optimization framework that couples system-level multi-objective optimization with an inner-loop MPPT mechanism.

A. Hierarchical Coupling and Evaluation Flow

For a fixed $\mathbf{x}$, the system is evaluated over an operating horizon $[0, T]$. At each time step, the tracker states are updated according to the tracking/control laws implied by $\mathbf{x}$, and the tracking error metric is computed using the solar AOI relationship in (1). Meanwhile, the inner-loop MPPT controller updates the converter duty cycle to maximize instantaneous PV power under the current operating condition, producing a power time series $P(t;\mathbf{x})$. The objective vector $\mathbf{f}(\mathbf{x}) = [f_1(\mathbf{x}), f_2(\mathbf{x}), f_3(\mathbf{x})]$ is then obtained using (2) and (4). This evaluation process is repeatedly called by the outer-loop multi-objective optimizer to approximate the Pareto set of (5).

B. Inner-Loop MPPT Problem Formulation

The inner-loop MPPT is formulated as a constrained one-dimensional optimization problem over the DC-DC converter duty cycle $d \in [d_{\min}, d_{\max}]$. At a given time instant, the instantaneous PV power is denoted by $P(d)$, and the MPPT objective is

$$d^\star = \arg\max_{d\in[d_{\min},d_{\max}]} P(d). \tag{6}$$

Under dynamic irradiance and partial shading, the power–voltage characteristic can become multi-modal, and conventional hill-climbing MPPT methods may exhibit oscillations or become trapped near local maxima. Population-based search is therefore adopted for improved robustness.

C. Chaotic Artificial Bee Colony (CABC) for MPPT

Artificial Bee Colony (ABC) is a population-based optimization method that models the foraging behavior of honey bees. In the MPPT setting, each food source corresponds to a candidate duty cycle d_i, and its quality (fitness) is evaluated by the measured or simulated PV power $P(d_i)$. The population $\{d_i\}_{i=1}^N$ is iteratively refined through employed-bee and onlooker-bee neighborhood searches, together with a scout mechanism that reintroduces diversity when progress stalls.

In standard ABC, a neighbor candidate $\tilde{d}_i$ is generated by

$$\tilde{d}_i = d_i + \phi\,(d_i - d_j), \qquad j \neq i, \tag{7}$$

where j is a randomly selected index and $\phi \in (-1, 1)$ controls the exploration step. The candidate is projected to satisfy duty-cycle bounds:

$$\tilde{d}_i \leftarrow \min\big(d_{\max}, \max(d_{\min}, \tilde{d}_i)\big). \tag{8}$$

Greedy selection is applied: $\tilde{d}_i$ replaces d_i if $P(\tilde{d}_i) > P(d_i)$. A trial counter is maintained for each food source; once it exceeds a predefined limit, the food source is abandoned and reinitialized by the scout phase.

To enhance exploration and mitigate premature convergence under multi-modal landscapes induced by partial shading, a chaotic sequence is incorporated to drive the update coefficient ϕ in (7). A chaotic state $z_k \in (0,1)$ is generated by a deterministic map:

$$z_k = \mu z_{k-1}(1 - z_{k-1}), \qquad z_k \in (0,1), \tag{9}$$

where μ controls the chaotic dynamics (typically near 4). The exploration coefficient is then defined as

$$\phi = 2z_k - 1, \tag{10}$$

so that $\phi \in (-1,1)$ while providing non-periodic bounded perturbations. Compared with purely random coefficients, the chaotic-driven update promotes more diversified search behavior, which is beneficial for MPPT under partial shading where multiple local maxima may exist. The resulting CABC-based MPPT procedure is summarized in Algorithm 1.

Algorithm 1: Inner-loop CABC-based MPPT

Input: Bounds $[d_{\min}, d_{\max}]$; population size N; scout limit $\mathcal{L}$; max iterations K; chaotic parameter μ
Output: Estimated MPP duty cycle $d^\star$

Initialize $\{d_i\}_{i=1}^N$ uniformly in $[d_{\min}, d_{\max}]$ Evaluate $P(d_i)$ and set $\text{trial}_i \leftarrow 0$ for all i;
Initialize $z_0 \in (0,1)$; `// chaotic state`
for $k \leftarrow 1$ **to** K **do**
  Update chaotic state $z_k \leftarrow \mu z_{k-1}(1 - z_{k-1})$; `// logistic map`
  Set $\phi \leftarrow 2z_k - 1$; `//` $\phi \in (-1,1)$ `controls step size`
  for $i \leftarrow 1$ **to** N **do**
    Randomly select $j \neq i$;
    $\tilde{d}_i \leftarrow d_i + \phi(d_i - d_j)$; `// neighbor search`
    $\tilde{d}_i \leftarrow \min(d_{\max}, \max(d_{\min}, \tilde{d}_i))$; `// projection`
    Evaluate $P(\tilde{d}_i)$;
    if $P(\tilde{d}_i) > P(d_i)$ **then**
      $d_i \leftarrow \tilde{d}_i$; $\text{trial}_i \leftarrow 0$; `// greedy selection`
    else
      $\text{trial}_i \leftarrow \text{trial}_i + 1$;
  for $i \leftarrow 1$ **to** N **do**
    if $\text{trial}_i \geq \mathcal{L}$ **then**
      Reinitialize d_i uniformly in $[d_{\min}, d_{\max}]$; `// scout re-diversification`
      Evaluate $P(d_i)$; $\text{trial}_i \leftarrow 0$;
$d^\star \leftarrow \arg\max_{i \in \{1,\dots,N\}} P(d_i)$
return $d^\star$;

D. Outer-Loop System-Level Multi-Objective Optimization

The outer-loop optimizer searches for $\mathbf{x} \in \Omega$ that minimizes the objective vector $\mathbf{f}(\mathbf{x})$ in (5). For each candidate $\mathbf{x}$, a closed-loop evaluation is performed over $[0, T]$: (i) the tracker motion and control response are determined by $\mathbf{x}$; (ii) the AOI-based tracking metric is computed using (1) to evaluate $f_2(\mathbf{x})$; (iii) the embedded inner-loop MPPT (Algorithm 1) updates the duty cycle to generate $P(t; \mathbf{x})$ and thus evaluate $f_1(\mathbf{x})$; and (iv) control effort and stability are quantified to obtain $f_3(\mathbf{x})$.

A multi-objective evolutionary optimization algorithm is then employed to approximate the Pareto-optimal set of (5). The resulting non-dominated solutions explicitly characterize trade-offs among power generation, tracking accuracy, and control effort, enabling practical operating-point selection according to deployment priorities (e.g., maximum energy yield versus reduced actuator usage). In the experimental section, Pareto fronts are analyzed to interpret system-level performance limits and guide the selection of representative operating strategies for the portable multi-axis solar tracking prototype.

V. Experiment and Comparison Results

A. Inner-Loop MPPT Benchmarking Under Dynamic and Shaded Conditions

This experiment isolates the effectiveness of the proposed inner-loop CABC-based MPPT in maximizing instantaneous PV power. Two PV models are used to test robustness with respect to modeling fidelity: (a) an idealized simple model for fast evaluation, and (b) a single-diode model (SDM) that better captures PV I-V behavior (including the influence of resistive effects) under varying irradiance and partial shading. The MPPT task is formulated as duty-cycle search within fixed bounds, and each compared optimizer returns a duty cycle that maximizes the resulting power. For fair comparison, all algorithms operate under the same duty-cycle bounds and termination criteria, and CPU time is reported as the execution time for a single MPPT run under the specified setting.

TABLE I
MPPT benchmarking results for duty-cycle search under two PV models

Algorithm	Duty Cycle	Power (W)	CPU (ms)
Simple Model			
ABC	0.80	144.00	0.134
ACO	0.85	141.24	0.628
PSO	0.90	151.20	0.029
GA	0.90	151.20	0.123
CABC	**0.97**	**165.53**	0.750
Single Diode Model			
ABC	0.90	142.16	0.204
ACO	0.88	145.05	1.990
PSO	0.90	142.16	0.047
GA	0.90	142.16	0.165
CABC	**0.92**	**144.87**	0.456

Table I summarizes the achieved duty cycle, output power, and CPU time across the compared swarm baselines (ABC, ACO, PSO, and GA) and the proposed CABC. Best results in each model block are highlighted in bold. Overall, CABC consistently attains strong solutions across both PV models, indicating improved exploration ability in the duty-cycle domain. Relative to standard ABC, the chaotic enhancement helps maintain search diversity and stabilizes convergence in challenging operating conditions (e.g., multi-modal landscapes induced by partial shading), which supports the use of CABC as the embedded inner-loop optimizer for the power objective $f_1(\mathbf{x})$ in (2).

B. Control-Performance Studies via PID Fine-Tuning

This experiment examines how controller tuning influences tracking dynamics, stability, and power consistency, which directly relates to the tracking-performance and control-effort objectives defined in (3) and (4). Three PID gain search ranges are considered to reflect different design preferences (aggressive tracking versus conservative/stable motion). Fig. 2 visualizes representative closed-loop responses and the corresponding duty-cycle outputs for two gain ranges, and Fig. 3 compares the resulting power outputs. Table II reports quantitative metrics, including rise time (RT), settling time (ST), overshoot (O), and steady-state error (SSE), together with the optimized PID gains.

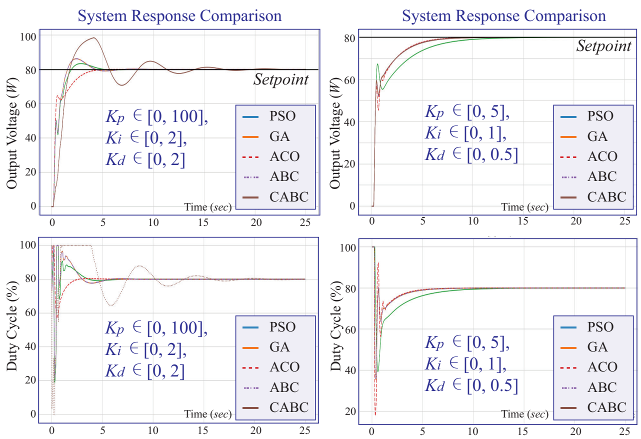

Fig. 2. Closed-loop response and duty-cycle outputs under different PID gain ranges. The left and right panels compare two representative search ranges, illustrating how gain constraints affect transient response and duty-cycle behavior.

TABLE II

PID FINE-TUNING RESULTS UNDER THREE GAIN SEARCH RANGES. LOWER RT, ST, OVERSHOOT, AND |SSE| INDICATE IMPROVED TRANSIENT PERFORMANCE AND REDUCED STEADY-STATE ERROR.

Alg.	RT (*sec*)	ST (*sec*)	O (%)	SSE	K_p	K_i	K_d
(a) Range: $K_p \in [0, 10]$, $K_i \in [0, 10]$, $K_d \in [0, 10]$							
PSO	0.8103	18.18	23.28	-0.008	0.00	3.72	0.45
GA-DE	0.8103	18.18	23.28	-0.009	0.00	3.72	0.45
ACO	0.3902	5.39	18.37	18.73	1.06	4.49	0.24
ABC	0.8103	18.18	23.28	-0.037	0.00	3.71	0.45
CABC	0.8003	18.07	**23.30**	0.277	0.00	**3.83**	**0.45**
(b) Range: $K_p \in [0, 100]$, $K_i \in [0, 2]$, $K_d \in [0, 2]$							
PSO	0.9804	3.80	7.70	0.00	0.87	2.00	0.29
GA-DE	0.9804	3.80	7.70	0.00	0.87	2.00	0.29
ACO	1.8810	3.61	0.03	0.00	1.11	1.35	0.04
ABC	0.9804	3.81	7.70	0.00	0.87	2.00	0.29
CABC	**1.1810**	**13.31**	**22.97**	0.043	0.00	2.00	**0.45**
(c) Range: $K_p \in [0, 5]$, $K_i \in [0, 1]$, $K_d \in [0, 0.5]$							
PSO	2.6110	5.80	0.00	0.00	1.48	1.00	0.19
GA-DE	2.6110	5.77	0.00	0.00	1.47	1.00	0.19
ACO	2.5810	5.59	0.00	0.00	1.40	0.98	0.24
ABC	2.6110	5.79	0.00	0.00	1.48	1.00	0.19
CABC	**2.6210**	**5.88**	0.00	0.00	**1.51**	**1.00**	0.19

The results indicate that gain ranges materially affect transient behavior and stability. In particular, tuning that improves transient response and reduces tracking error may increase control activity and can introduce larger oscillations, which are penalized by $f_3(\mathbf{x})$. Conversely, more conservative tuning can reduce overshoot and control effort but may slow response. These observations emphasize why solar tracking should be treated as a system-level problem: optimizing power alone is insufficient without accounting for tracking performance and control-related trade-offs.

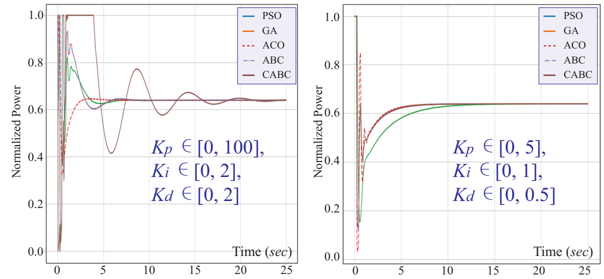

Fig. 3. Power output comparison under two PID gain search ranges. The curves illustrate how tracking-control tuning influences power consistency through its impact on tracking dynamics.

C. System-Level Multi-Objective Trade-Off Analysis and Hardware Validation

This experiment evaluates the proposed *system-level* multi-objective formulation in (5) under closed-loop operation. Each candidate decision vector $\mathbf{x}$ is simulated with the embedded CABC-based MPPT running online, so the resulting objective values reflect the coupled behavior of tracking dynamics, actuator usage, and real-time power optimization rather than an idealized power model. Instead of reporting only a single best configuration, the multi-objective setting produces a set of non-dominated operating strategies that expose design trade-offs relevant to portable multi-axis trackers.

TABLE III

OBJECTIVE DEFINITIONS AND DIRECTIONALITY FOR INTERPRETING SYSTEM-LEVEL TRADE-OFFS.

Objective	Definition	Unit	Preferred
$f_1(\mathbf{x})$	$-\frac{1}{T}\int_0^T P(t;\mathbf{x})\,dt$	W (avg.)	lower $\Rightarrow$ higher power
$f_2(\mathbf{x})$	$\frac{1}{T}\int_0^T \alpha(t;\mathbf{x})\,dt$	deg	lower
$f_3(\mathbf{x})$	$\frac{1}{T}\int_0^T \lVert u(t;\mathbf{x})\rVert^2\,dt$	(a.u.)	lower

To make the multi-objective results unambiguous to readers, Table III summarizes the objectives and their preferred directions. Although the optimization is posed as minimization in (5), the energy objective is expressed as a cost-form term (negative average harvested power), so that lower f_1 corresponds to *higher* harvested power. Meanwhile, lower f_2 and f_3 correspond to improved alignment (smaller AOI loss) and reduced control effort, respectively. The non-dominated set demonstrates the expected coupling among objectives: configurations that increase harvested power (lower f_1) typically require tighter pointing (lower f_2) and/or more aggressive actuation (higher control activity, increasing f_3). Practically, the benefit of the multi-objective formulation is that it supports *operating-point selection* according to deployment priorities: (a) an energy-prioritized setting that favors lower f_1 when maximizing yield is the primary goal; (b) a stability/actuator-prioritized setting that favors lower f_3 when actuator usage, wear, or power budget for motion is constrained; and (c) a balanced setting near the “knee” region that provides strong harvested power without excessive control effort.

Hardware experiments are further conducted on a portable multi-axis solar tracking prototype to validate practical feasibility. The prototype integrates multi-axis actuation and a PV panel, enabling real-world alignment under natural sunlight. Fig. 4 shows representative operating configurations. The same hierarchical logic is executed in practice: the tracker performs orientation adjustment while the inner-loop CABC-based MPPT updates the converter duty cycle online. Hardware observations confirm that the proposed framework can be executed on a portable platform. Moreover, improved alignment together with stable control behavior is associated with higher and more consistent power output, which is consistent with the system-level coupling.

(a) (b) (c)

Fig. 4. Portable multi-axis solar tracking prototype for hardware validation. (a) Tracker raised by the linear actuator. (b) Actuation and mounting structure connecting the PV panel to the tripod (DC motor on the arm and stepper motor at the base). (c) Prototype oriented toward incident sunlight from a different viewing angle, illustrating multi-axis alignment capability.

VI. Conclusion

In this paper, solar tracking was formulated as a system-level multi-objective optimization problem that jointly considers energy yield, tracking performance, and control effort under practical constraints. A hierarchical optimization framework was developed in which a CABC-based MPPT strategy was embedded as the inner-loop power optimizer, enabling closed-loop evaluation of the power objective under dynamic and partially shaded conditions. Experimental results from simulations and hardware validation demonstrate that the proposed framework provides explicit Pareto trade-offs and supports robust operating-point selection for portable multi-axis solar tracking. Future work will focus on extending the framework to broader environmental uncertainties and real-time adaptive selection of Pareto-optimal operating strategies.

References

[1] S. Habib, H. Liu, M. Tamoor, M. A. Zaka, Y. Jia, A. G. Hussien, H. M. Zawbaa, and S. Kamel, "Technical modelling of solar photovoltaic water pumping system and evaluation of system performance and their socio-economic impact," *Heliyon*, vol. 9, no. 5, 2023.

[2] N. Kuttybay, S. Mekhilef, N. Koshkarbay, A. Saymbetov, M. Nurgaliyev, G. Dosymbetova, S. Orynbassar, E. Yershov, A. Kapparova, B. Zholamanov *et al.*, "Assessment of solar tracking systems: A comprehensive review," *Sustainable Energy Technologies and Assessments*, vol. 68, p. 103879, 2024.

[3] K. Kumar, L. Varshney, A. Ambikapathy, R. K. Saket, and S. Mekhilef, "Solar tracker transcript—a review," *International Transactions on Electrical Energy Systems*, vol. 31, no. 12, p. e13250, 2021.

[4] T. Lei, C. Luo, G. E. Jan, and Z. Bi, "Deep learning-based complete coverage path planning with re-joint and obstacle fusion paradigm," *Frontiers in Robotics and AI*, vol. 9, 2022.

[5] A. Diaz, R. Garrido, and J. Soto-Bernal, "A filtered sun sensor for solar tracking in HCPV and CSP systems," *IEEE Sensors Journal*, vol. 19, no. 3, pp. 917–925, 2018.

[6] T. Lei, C. Luo, J. E. Ball, and Z. Bi, "A hybrid fireworks algorithm to navigation and mapping," in *Handbook of Research on Fireworks Algorithms and Swarm Intelligence*. IGI Global, 2020, pp. 213–232.

[7] C. Jamroen, C. Fongkerd, W. Krongpha, P. Komkum, A. Pirayawaraporn, and N. Chindakham, "A novel UV sensor-based dual-axis solar tracking system: Implementation and performance analysis," *Applied Energy*, vol. 299, p. 117295, 2021.

[8] C. Morón, D. Ferrández, P. Saiz, G. Vega, and J. P. Díaz, "New prototype of photovoltaic solar tracker based on arduino," *Energies*, vol. 10, no. 9, p. 1298, 2017.

[9] A. Ammar, K. Hamraoui, M. Belguellaoui, and A. Kheldoun, "Performance enhancement of photovoltaic water pumping system based on bldc motor under partial shading condition," *Engineering Proceedings*, vol. 14, no. 1, p. 22, 2022.

[10] D. Sooriamoorthy, A. Manoharan, S. K. Sivanesan, S. K. Lun, A. C. H. Cheong, and S. K. S. Perumal, "Optimizing solar maximum power point tracking with adaptive PSO: A comparative analysis of inertia weight and acceleration coefficient strategies," *Results in Engineering*, p. 106429, 2025.

[11] T. Sellers, T. Lei, G. E. Jan, Y. Wang, and C. Luo, "Multi-objective optimization robot navigation through a graph-driven PSO mechanism," in *Advances in Swarm Intelligence: 13th International Conference, ICSI 2022, Xi'an, China, July 15–19, 2022, Proceedings, Part II*. Springer, 2022, pp. 66–77.

[12] T. Lei, T. Sellers, C. Luo, L. Cao, and Z. Bi, "Digital twin-based multi-objective autonomous vehicle navigation approach as applied in infrastructure construction," *IET Cyber-Systems and Robotics*, vol. 6, no. 2, p. e12110, 2024.

[13] T. Lei, C. Luo, S. X. Yang, D. W. Carruth, and Z. Bi, "Bio-inspired intelligence-based multi-agent navigation with safety-aware considerations," *IEEE Transactions on Artificial Intelligence*, vol. 5, no. 6, pp. 2946–2961, 2024.

[14] T. Lei, P. Chintam, D. W. Carruth, G. E. Jan, and C. Luo, "Human-autonomy teaming-based robot informative path planning and mapping algorithms with tree search mechanism," in *IEEE International Conference on Human-Machine Systems (ICHMS)*. IEEE, 2022, pp. 1–6.

[15] N. Zhao, J. Zhang, Y. Dong, and C. Ding, "Multi-objective optimization and sensitivity analysis of building envelopes and solar panels using intelligent algorithms," *Buildings*, vol. 14, no. 10, p. 3134, 2024.

[16] T. Lei, C. Luo, J. E. Ball, and S. Rahimi, "A graph-based ant-like approach to optimal path planning," in *2020 IEEE Congress on Evolutionary Computation (CEC)*. IEEE, 2020, pp. 1–6.

[17] B. Black, T. Sellers, T. Lei, C. Luo, and D. W. Carruth, "Optimal multi-target navigation via graph-based algorithms in complex environments," in *2024 IEEE 33rd International Symposium on Industrial Electronics (ISIE)*. IEEE, 2024, pp. 1–6.

[18] T. Lei, T. Sellers, C. Luo, and L. Zhang, "A bio-inspired neural network approach to robot navigation and mapping with nature-inspired algorithms," in *Advances in Swarm Intelligence: 13th International Conference, ICSI 2022, Xi'an, China, July 15–19, 2022, Proceedings, Part II*. Springer, 2022, pp. 3–16.

[19] T. Sellers, T. Lei, C. Luo, G. E. Jan, and J. Ma, "A node selection algorithm to graph-based multi-waypoint optimization navigation and mapping," *Intelligence & Robotics*, vol. 2, no. 4, pp. 333–54, 2022.

[20] T. Lei, C. Luo, T. Sellers, and S. Rahimi, "A bat-pigeon algorithm to crack detection-enabled autonomous vehicle navigation and mapping," *Intelligent Systems with Applications*, vol. 12, p. 200053, 2021.

[21] D. Short, T. Lei, D. W. Carruth, C. Luo, and Z. Bi, "A bio-inspired algorithm in image-based path planning and localization using visual features and maps," *Intelligence & Robotics*, vol. 3, no. 2, pp. 222–41, 2023.

[22] S. Steen, T. Lei, C. Luo, S. Shao, and L. Gong, "A moss growth optimization approach to robot path planning," in *2025 IEEE Congress on Evolutionary Computation (CEC)*. IEEE, 2025, pp. 1–4.

[23] M. Hicks, T. Lei, C. Luo, L. Liu, and Z. Bi, "A bio-inspired goal-directed cognitive map approach to robot navigation and mapping," in *2025 IEEE Congress on Evolutionary Computation (CEC)*. IEEE, 2025, pp. 1–8.

[24] T. Lei, T. Sellers, C. Luo, D. W. Carruth, and Z. Bi, "Graph-based robot optimal path planning with bio-inspired algorithms," *Biomimetic Intelligence and Robotics*, p. 100119, 2023.

[25] T. Sellers, T. Lei, C. Luo, Z. Bi, and G. E. Jan, "Human autonomy teaming-based safety-aware navigation through bio-inspired and graph-based algorithms," *Biomimetic Intelligence and Robotics*, vol. 4, no. 4, p. 100189, 2024.